



# Proteome and phospholipid alteration reveal metabolic network of *Bacillus thuringiensis* under triclosan stress



Yi Li<sup>a</sup>, Chongshu Li<sup>a</sup>, Huaming Qin<sup>a</sup>, Meng Yang<sup>a</sup>, Jinshao Ye<sup>a,b,\*</sup>, Yan Long<sup>a</sup>, Huase Ou<sup>a</sup>

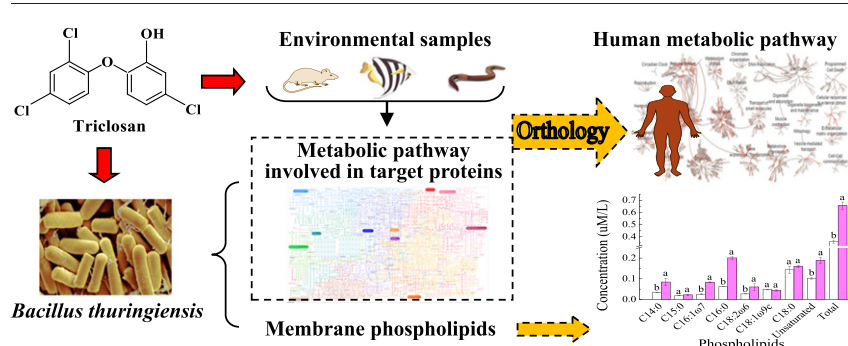
<sup>a</sup> Key Laboratory of Environmental Exposure and Health of Guangdong Province, School of Environment, Jinan University, Guangzhou 510632, China

<sup>b</sup> Joint Genome Institute, Lawrence Berkeley National Laboratory, Walnut Creek 94598, CA, USA

## HIGHLIGHTS

- Cell metabolism under triclosan stress at pathway and network levels was explored.
- PyrH and Eno would be biomarkers to reflect triclosan stress.
- Glycolysis and pyruvate metabolism were inhibited by triclosan.
- Ten proteins responded to triclosan stress were mapped in human metabolic network.
- Omics approach was developed to evaluate the safety of target compounds.

## GRAPHICAL ABSTRACT



## ARTICLE INFO

### Article history:

Received 30 July 2017

Received in revised form 30 September 2017

Accepted 1 October 2017

Available online 5 October 2017

Editor: Jay Gan

### Keywords:

Triclosan  
Phospholipid  
Biomarker  
Metabolism network  
Proteomics  
Homology

## ABSTRACT

Triclosan is a common antibacterial agent widely applied in various household and personal care products. The molecule, cell, organ and organism-level understanding of its toxicity pose to some target organisms has been investigated, whereas, the alteration of a single metabolic reaction, gene or protein cannot reflect the impact of triclosan on metabolic network. To clarify the interaction between triclosan stress and metabolism at network and system levels, phospholipid synthesis, and cellular proteome and metabolism of *Bacillus thuringiensis* under 1  $\mu\text{M}$  of triclosan stress were investigated through omics approaches. The results showed that C14:0, C16:1 $\omega$ 7, C16:0 and C18:2 $\omega$ 6 were significantly up-produced, and 19 proteins were differentially expressed. Whereas, energy supply, protein repair and the synthesis of DNA, RNA and protein were down-regulated. PyrH and Eno could be biomarkers to reflect triclosan stress. At network level, the target proteins ACOX1, AHR, CAR, CYP1A, CYP1B1, DNMT1, ENO, HSP60, HSP70, SLC5A5, TPO and UGT expressed in different species shared high sequence homology with the same function proteins found in *Homo sapiens* not only validated their role as biomarkers but also implied the potential impact of triclosan on the metabolic pathways and network of humans. These findings provided novel insights into the metabolic influence of triclosan at network levels, and developed an omics approach to evaluate the safety of target compound.

© 2017 Published by Elsevier B.V.

## 1. Introduction

As an antimicrobial agent and bactericide with a broad spectrum of antimicrobial activity, triclosan is widely used in personal care products, medical supplies and household cleaning products. Triclosan easily enters the natural environments through wastewater discharge and has been

\* Corresponding author at: Key Laboratory of Environmental Exposure and Health of Guangdong Province, School of Environment, Jinan University, Guangzhou 510632, China.  
E-mail address: [jsye@jnu.edu.cn](mailto:jsye@jnu.edu.cn) (J. Ye).

detected in most of the environmental samples due to its widespread use and incomplete removal from wastewater treatment plants (Amariei et al., 2017). For decades accumulation in natural ecosystems, its concentration in the aquatic environments, sediments and biosolids is up to  $26.8 \mu\text{g}\cdot\text{L}^{-1}$ ,  $800 \mu\text{g}\cdot\text{kg}^{-1}$  and  $30 \text{mg}\cdot\text{kg}^{-1}$ , respectively (Dann and Hontela, 2011).

The biological toxicity and potential influences of triclosan on some species have been investigated. For example, in mammals, triclosan acted as an endocrine disruptor that reduced the expression of enzymes in thyroid hormone of rat and further affected brain development (Axelstad et al., 2013). For aquatic organisms, triclosan showed a potential risk against hemocytes of the marine gastropod *Haliotis tuberculata* (Gaume et al., 2012). At a concentration of  $1 \mu\text{M}$ , it could fluctuate the lysosomal membrane of the mussel *Mytilus galloprovincialis* (Canesi et al., 2007). For bacterial, triclosan could disrupt the stability of bacterial membranes, leading to structural disturbances and loss of permeability barriers (Phan and Marquis, 2006). At molecular level, triclosan was found block bacterial fatty acid synthesis via inhibiting acyl carrier protein reductase (Levy et al., 1999). It was also reported that triclosan induced the transcriptional regulation of *fabI*, an efflux pump in *Pseudomonas*, and posed influences on the transport of substituted acyl-CoA reductase in *Alcaligenes xylosoxidans* (Meade et al., 2001).

However, each metabolic reaction, gene or protein is only a single node in a complicated metabolic network. The differentially expressed regulation of a single biomolecule does not imply the corresponding alteration of the related pathway or network. Omics aims at the collective characterization, function and quantification of all biomolecules produced in target cells or organisms (Mayer et al., 2011). It could be an insightful approach to reveal global metabolic response of organisms under various stresses. To clarify the interaction between triclosan stress and cellular metabolism at network and system levels, and develop an omics approach to evaluate the toxicity of target compounds, the current study would investigate the protein, phospholipid and metabolism response of target organism to triclosan stress using proteomics and lipidomics technologies. Triclosan is a chlorinated aromatic compound that has functional groups representative of both ethers and phenols. The potential findings related to its omics responses will present an insightful reference to the compounds with the same functional groups.

The Gram-positive bacterium *Bacillus thuringiensis* is famous for forming insecticidal crystal proteins, which have highly toxic effect to some susceptible insects (Treitz et al., 2015). In insect midgut, crystal proteins can activate cellular signaling thereby lead to cell death by binding the midgut cadherin-like protein (Zhang et al., 2005). Due to this insecticidal effect, *B. thuringiensis* has been widely used as a biopesticide employed in agriculture (van Frankenhuyzen, 2009). Moreover, *B. thuringiensis* owns unique gene families related to the degradation of pollutants (Tang et al., 2016) and the regulation of complicated metabolic network under a wide range of environmental fluctuations (de Been et al., 2006). Therefore, it would be a perfect modal microbe for investigating the metabolic network response of cells under triclosan stress.

The aim of this work is to explore the interaction between triclosan stress, protein interaction and cellular metabolism of *B. thuringiensis* at pathway and network levels. To this end, the membrane potential, phospholipids and proteome expression of *B. thuringiensis* under triclosan stress were investigated through flow cytometry, gas chromatography-mass spectroscopy and Sciex Triple TOF 5600 mass spectrometer analysis. The metabolic impact of triclosan on the different species and human was also studied through phylogenetic and reactomic approaches. The findings would provide novel insights into the metabolic influence of triclosan on cells at system and network levels.

## 2. Materials and methods

### 2.1. Strain and chemicals

*B. thuringiensis* GIMCC1.817 was an effective microbe for the degradation of multi-pollutants and was stored at the Microbiology Culture

Centre of Guangdong Province, China. Triclosan (CAS registration number 3380-34-5) was purchased from Sigma-Aldrich (St. Louis, MO, USA), and was dissolved in the chromatographic grade of methanol to prepare a stock solution at  $1 \text{g}\cdot\text{L}^{-1}$ . Lysogeny broth used for cell culture contained (in  $\text{g}\cdot\text{L}^{-1}$ ) 5 beef extract, 5 NaCl and 10 peptone. The treatment medium for cellular exposure to triclosan contained (in  $\text{g}\cdot\text{L}^{-1}$ ) 0.03 beef extract, 0.1 peptone, 0.07 NaCl, 0.03  $\text{KH}_2\text{PO}_4$ , 0.03  $\text{NH}_4\text{Cl}$  and 0.01  $\text{MgSO}_4$ , respectively.

### 2.2. Microbial culture and triclosan treatment

The cells of *B. thuringiensis* GIMCC1.817 were inoculated into lysogeny broth medium and cultured at  $100 \text{r}\cdot\text{min}^{-1}$  on a rotary shaker at  $30^\circ\text{C}$  for 12 h. After separation from the medium by centrifugation at  $1300 \times \text{g}$ , the cells were washed three times by sterile phosphate buffer (pH 7.4).

The washed cells were then used to prepare a cellular suspension by adding sterile phosphate buffer. Immediately, the bacterial suspension was added to the treatment medium at the final biomass of  $1.5 \times 10^{12}$  colony-forming unit. Subsequently, the triclosan stock solution at  $1 \text{g}\cdot\text{L}^{-1}$  was pipetted into the treatment medium, in which the initial concentration of triclosan was  $1 \mu\text{M}$ . All samples were cultured in the dark at  $30^\circ\text{C}$  on a rotary shaker at  $100 \text{r}\cdot\text{min}^{-1}$ . The cells in two groups of samples were collected in 0, 5, 12, 18 and 24 h, respectively, and were utilized to measure membrane potential. In addition, the cells in two groups of samples collected in 24 h were used to extract phospholipids, proteins and RNA.

### 2.3. Analysis of membrane potential

The BD™ MitoScreen kit (BD, San Jose, US), which consists of lyophilized JC-1 reagent, dimethyl sulfoxide (DMSO) and 10-fold assay buffer, was designed for use in flow cytometry. Briefly, the lyophilized JC-1 reagent was dissolved at room temperature with  $125 \mu\text{L}$  DMSO per vial to yield a JC-1 stock solution. The 1-fold assay buffer was prepared by diluting the 10-fold assay buffer in deionized water. Next, the JC-1 dye solution was prepared by diluting the JC-1 stock solution 1:100 with 1fold assay buffer.

After the collected cells were suspended in  $200 \mu\text{L}$  of JC-1 dye solution, all the samples were incubated at  $25^\circ\text{C}$  for 15 min in a dark place. Subsequently, the stained cells were pipetted to tubes with BD CaliBRITE™ beads and analyzed by FACS Aria flow cytometer (BD, USA). Briefly, 10,000 cells of each sample were analyzed by the laser beam at the excitation wavelength of 488 nm individually. The detector measured emission intensity was set at 605 to 625 nm. For each cell, the scattered light was detected by a photo diode at 2 different positions (forward and side scattered light) and converted into electric signals and fluorescence intensity. The JC-1 monomers emitted green fluorescence, whereas, the aggregates emitted red fluorescence. These two kinds of fluorescence were captured through 527 and 590 nm long-pass filters, respectively. The mean values of three parallel samples were statistically analyzed by SPSS version 17.0 using the one-way ANOVA method.

### 2.4. Extraction and determination of membrane phospholipids

The extraction method of phospholipids was referred to reference (Yang et al., 2017). After extraction, phospholipids were analyzed using gas chromatograph tandem mass spectrometer (GC-MS) (SHIMADZU GCMS-QP 2010 Ultra) equipped with a DB-5MS ( $30 \text{m} \times 0.25 \text{mm} \times 0.25 \mu\text{m}$ ) quartz capillary column. The condition of GC-MS analysis was as follows: the column temperature was  $140^\circ\text{C}$ , remained 2 min and heated to  $260^\circ\text{C}$  at a rate of  $3^\circ\text{C}\cdot\text{min}^{-1}$ . The carrier gas was He. The sample inlet temperature and ion source temperature were set to  $250^\circ\text{C}$  and  $230^\circ\text{C}$ , respectively. The mass spectrometry scanning range was  $50\text{--}500 \text{m}\cdot\text{z}^{-1}$ . Quantification of phospholipids was used

peak area and internal standard curve method. All of the experiments were performed in triplicate, and the mean values were used in the *t*-test calculations.

### 2.5. Extraction and digestion of proteins

The extraction and digestion of cellular proteins were based on the published method (Ye et al., 2017). Briefly, the cells before and after exposure to triclosan were suspended in 1 mL lysis buffer (15 mM Tris-HCl, 7 M urea, 2 M thiourea, 1% w/v DTT, 4% w/v CHAPS) added with  $0.2 \text{ g} \cdot \text{L}^{-1}$  phenyl methyl sulfonyl fluoride, 2% v/v IPG buffer and  $0.6 \text{ g} \cdot \text{L}^{-1}$  DTT. After vibration thrice with 10s per time, the samples were frozen in liquid nitrogen for 15 min, followed by ultrasonication for 20 min. Benzoylase nuclease (HaiGene, C2001) at 25 KU was added to the lysate at a final concentration of 1% v/v mixture, and incubated at 4 °C for 30 min. Subsequently, the cell debris was removed at 4 °C by centrifugation at  $16700 \times g$  for 1 h. Protein concentrations were determined using the Bradford (Silverio et al., 2012).

The obtained 100 µg proteins from each sample were reduced by 2 µL of 54.4 mM tris (2-carboxyethyl) phosphine (AB Sciex, Framingham, USA) at 37 °C for 1 h. The cysteines were blocked with 1 µL cysteine-blocking reagent for 10 min at room temperature. The protein samples were then centrifuged using 10 KD Amicon Ultra-0.5 filters at  $13200 \times g$  for 20 min and washed three times with 100 µL dissolution buffer (pH 8.5) (AB Sciex, Framingham, USA), which mainly consisted of 1 M tetraethylammonium bromide. The samples in filter devices were digested overnight using 50 µL dissolution buffer contained 2 µg of trypsin (Promega, V5280, USA) at 37 °C after removal of the liquid collected in tube. Subsequently, the released peptides were collected by centrifugation at  $13200 \times g$  for 20 min, followed by trypsin digestion in a washing ultrafiltration tube with 50 µL dissolution buffer for 2 h.

### 2.6. iTRAQ labeling and strong cation exchange fractionation.

The tryptic peptides were labeled with an iTRAQ reagent multiplex kit (Sigma, PN 4352135, US) according to the manufacturer's protocol (Ye et al., 2017). Briefly, the concentration of the collected peptides was detected by Bradford method and then the same amount of peptides was used for labeling. The control samples and those after exposure to triclosan were labeled with reagents 114, and 115, respectively. Ethanol at 150 µL was added to each tube of iTRAQ reagent, followed by vortex. After the tryptic peptides were transferred to a new tube, chromatographic-grade water at 100 µL was added to each sample to stop the reaction. One microliter of solution from each sample was detected by ABI 4800 MALDI TOF/TOF (Applied Biosystems, Foster City, CA) to determine the labeling efficiency. Subsequently, all the iTRAQ-labeled peptide mixtures were mixed, vortex, and then desalinated with Strata-X (Phenomenex, USA). Subsequently, peptides were eluted with solution (98% v/v ACN, 0.1% v/v formic acid), and detected by an AB Sciex Triple TOF 5600 mass spectrometer (AB SCIEX, Framingham, MA, USA) equipped with a Nanospray III source (AB SCIEX) using the following parameter settings: spray voltage, 2.3 kV; sheath gas (nitrogen) pressure, 30 psi; collision gas (nitrogen) pressure, 15 psi; vaporizer temperature, 120 °C. Survey scans were acquired in 250 ms, and up to 30 product ion scans were collected if they exceeded a threshold of 120 counts per second (counts/s) with a 2+ to 5+ charge-state. A sweeping collision energy setting of  $35 \pm 5 \text{ eV}$  coupled with iTRAQ adjusted rolling collision energy was applied to all precursor ions for collision-induced dissociation. Dynamic exclusion was set for half of the peak width (18 s), and the precursor was then refreshed off the exclusion list.

### 2.7. Protein identification and bioinformatic analysis

The data were searched in Mascot 2.2 (Matrix Science, Boston, MA, USA) for calculating the false discovery rate (FDR) of identified peptides.

The raw files were converted to MASCOT generic format (.mgf) files via Proteome Discoverer 1.4 software (Thermo Fisher Scientific) with default settings for proteome analysis. A strict cutoff with FDR < 1% and ion score < 0.05 (with 95% confidence) were set to minimize false positive results of protein identification.

The Universal Protein Resource (Uniprot, <http://www.uniprot.org>) was used to obtain gene ontology (GO) annotations of the identified proteins. The Database for Annotation, Visualization and Integrated Discovery (DAVID) 6.7 Bioinformatics tool (<http://david.abcc.ncifcrf.gov>) was used to analyze protein clustering. Moreover, the differentially expressed proteins (DEPs) were analyzed by PANTHER (<http://www.pantherdb.org>) to describe their biological process, cellular component, molecular function and protein class. For further exploring metabolic reaction network catalyzed by the identified enzymes, metabolic pathways were mapped out Kyoto Encyclopedia of Genes and Genomes (KEGG, <http://www.genome.jp/kegg/>) and REACTOME pathway database (<http://www.reactome.org/>). The interaction networks of all the identified proteins were assigned using the STRING database version 9.1.

### 2.8. Protein validation by qPCR

For total RNA extraction, the cells cultured for 24 h according to the above conditions were collected with centrifugation at  $8000 \times g$  for 2 min at 4 °C and washed three times by sterile phosphate buffer. Immediately, the collected cells were suspended in 1 mL TransZol Up reagent (TRANS®) for lysis. Next, the target total RNA was extracted according to the instructions of the TransZol Up plus RNA kit (TRANS®). In addition, the purity of RNA was detected by measuring the OD value on a nucleic acid detector. For determining the integrity of the total RNA extraction, 1 µL RNA sample was used to run gels through 1% agarose gel electrophoresis, followed by a gel imaging.

The 5-fold All-in-one RT MasterMix (with AccuRT Genomic DNA Removal Kit) (abm®) was used for genomic DNA removal and first-strand cDNA synthesis. In brief, 2 µL of 4-fold AccuRT reaction mix (abm®) and nuclease-free water were added into a PCR tube contained 2 µg extracted RNA followed by incubation at 25 °C for 5 min. After the addition of 2 µL 5-fold AccuRT Reaction stopper (abm®) and a reverse transcription reaction reagent (4 µL 5-fold All-in-One RT MasterMix and 6 µL nuclease-free water), the mixture was subsequently incubated at 25 °C for 10 min, and further incubated at 42 °C for 15 min.

The cDNA product was applied as a template in a standard qPCR. The primer sequence of the target protein was designed online on NCBI (<https://www.ncbi.nlm.nih.gov/>) and indicated in Table S4. The qPCR amplification was performed at 95 °C for 10 min, followed by 35 cycles at 95 °C for 15 s, and 35 cycles at 60 °C for 1 min by using a CFX96™ Real-time PCR system (BIO-RAD).

## 3. Results and discussion

### 3.1. Membrane potential

According to the sporulation cycle of *B. thuringiensis*, the membrane potential of the treatment samples and control samples at 0, 5, 12, 18 and 24 h was detected. The results showed that membrane potential at 5, 12 and 18 h reduced under the stress of triclosan, and did not recover until the spores matured at about 24 h (Figs. 1, S1). This finding implied that triclosan induced the depolarization in *B. thuringiensis* before spore maturation. With depolarization enhancement, the ion channels on the cell membrane were regulated to inhibit the outflow of intracellular  $\text{K}^+$  and the influx of extracellular  $\text{Na}^+$ , or to transport  $\text{K}^+$  into the cells (Bortner et al., 2001).

As an important component of the cell membrane, phospholipids perform an important role not only in maintaining the fluidity and stability of biological membranes, but also regulating cellular signal transduction, and thus affecting cell function. Studies have pointed out

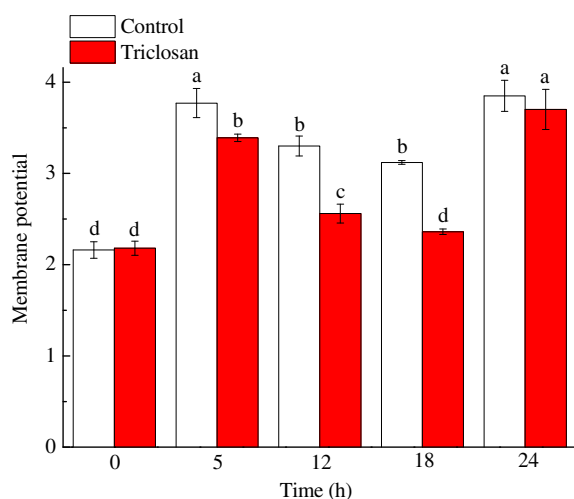


**Fig. 1.** Change of membrane potential of *B. thuringiensis* with time under triclosan stress. Control indicates the sample has no triclosan, and the same lowercase letter stands for no significant difference among the groups ( $P > 0.05$ ), different lowercase letter represents significant difference among the groups ( $P < 0.05$ ).

phospholipids can regulate ion channels through direct and indirect effects (Kim and Pleumsamran, 2000; Ordway et al., 1991). The direct pathway refers to the fact that phospholipids can interact with channel proteins or alter ionic channel activity. The indirect approach is that unsaturated phospholipids regulate ion channel activity through metabolic pathways, protein kinase pathways and other signaling pathways (Ordway et al., 1991). All these indicated that there was a definite relationship between membrane potential with membrane phospholipids and membrane proteins for controlling ion efflux and transport.

### 3.2. Phospholipid biosynthesis

In the control and treatment samples of this experiment, seven kinds of phospholipids were detected, including C14:0 (Myristic acid), C15:0 (Pentadecanoic acid), C16:1 $\omega$ 7 (Palmitoleic acid), C16:0 (Palmitic acid), C18:2 $\omega$ 6 (Linoleic acid), C18:1 $\omega$ 9 (Oleic acid) and C18:0 (Stearic

acid) (Fig. 2). The concentrations of myristic acid, palmitoleic acid, palmitic acid and linoleic acid were increased significantly in the treatment samples with triclosan. The unsaturation level was also raised in the treatment samples due to increase in the content of palmitoleic acid and linoleic acid.

Linoleic acid is a stress factor for many bacteria, resulting in inhibition of the cell growth and cytotoxicity of the cell membrane (Zheng et al., 2005). Linoleic acid has been proved to reduce  $K^+$  current through the protein kinase system in rat cells (Feng et al., 2006). Changes in phospholipid composition and membrane fluidity were proposed as a mechanism for the alteration of ion channel functions, and  $Na^+$ ,  $K^+$ -ATPase activity (Cornelius, 2001). Long chain phospholipids, especially myristic acid and linoleic acid, inhibited the  $Na^+$ ,  $K^+$ -ATPase (Morohashi et al., 1991). These meant that although the increase in phospholipid concentration induced by triclosan was harmful to cell growth, it could effectively inhibit the leakage of  $K^+$  and lead to repolarization of membrane potential. The specific regulation mechanism needed further analysis of proteome.

In addition, bacterial phospholipids synthesis is catalyzed by a series of independent enzymes, each of which catalyzes a specific reaction. The acyl carrier proteins are responsible for the translocation of acyl intermediates between enzymes. For functional proteins, malonyl-CoA, long-chain acyl-CoA synthetase, FabD, FabF, FabG, FabH, FabI and FabZ were involved in *B. thuringiensis* phospholipids synthesis.

### 3.3. Protein function and interaction

Among the 56 identified proteins (Table S1), 19 of them were significantly differential expressed with the ratios of the treatment samples higher than 1.2 or lower than 0.83 (Table S2). These DEPs were further classified by PANTHER Classification System into four subcategories, including biological process, cellular component, molecular function and protein classification (Fig. S2). Compared with down regulated proteins, the up-regulated ones were mainly ribosomal proteins. The functions of these ribosomal proteins were primarily involved in binding and structural molecular activity, which were linked to the structural proteins on the cell membrane and the formation of peptidoglycan.

For better understanding the metabolic function of the down-regulated proteins, all proteins obtained in this experiment (Table S1)

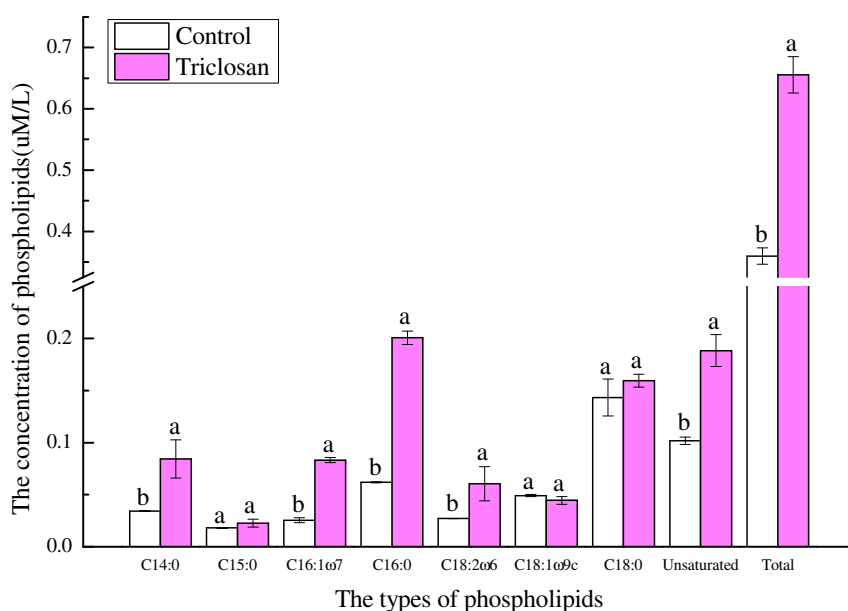


**Fig. 2.** Types and concentration of phospholipids in *B. thuringiensis* at 24 h. Control indicates the sample has no triclosan, and the same lowercase letter stands for no significant difference among the groups ( $P > 0.05$ ), different lowercase letter represents significant difference among the groups ( $P < 0.05$ ).

were clustered. Four main pathways, namely, ribosome, glycolysis, citrate cycle and pyrimidine metabolism, were mapped in the metabolism network with  $<0.05$   $p$ -value (Table S3, Fig. 3). In this network, glycolysis and pyruvate metabolism catalyzed by the down-regulated triosephosphate isomerase (TpiA), phosphopyruvate hydratase (Eno), branched-chain alpha-keto acid dehydrogenase subunit E2 (PdhC) and dihydrolipoamide dehydrogenase (PdhD) inferred triclosan depressed the central carbohydrate metabolism of *B. thuringiensis*. Based on the down-regulation of nucleoside diphosphate kinase (Ndk) and pyrimidine-nucleoside phosphorylase (Pdp) associated with pyrimidine metabolism, and dihydrolipoamide dehydrogenase (PdhD) participated in the TCA cycle, these two pathways were also suppressed (Fig. 3).

The protein-protein interaction analysis confirmed that the down-regulated proteins Eno, TpiA, PdhC, PdhD, DnaK, FusA, RplJ, PyrH and Ndk could enrich in an interaction network (Fig. 4). This finding revealed that some functional proteins with close relationship would show a global network response to triclosan stress. The molecular functions of these closely related proteins were further clarified.

Enolase (Eno) has been found to act as a membrane protein involved in the hydrogenation of polyunsaturated fatty acids and play an important role in cellular detoxification. For example, Eno in *Lactobacillus plantarum* participates in the complex hydrogenation of linoleic acid, which catalyzes the formation of conjugated linoleic acid and contributes to the virtuous cycle of intracellular metabolism (Ortega-Anaya and Hernandez-Santoyo, 2016). However, phospholipid (Fig. 2) results showed that Eno might not effectively alleviate the potential toxicity of linoleic acid to cells with the down-regulation of Eno and the up-production of linoleic acid in the current experiment. For another down-regulated protein TpiA in glycolysis, it has the function of catalyzing carbon nutrients for energy production or glycerol synthesis.

The pdhACD operons can transfer pyruvate into acetyl-CoA in the carbohydrate metabolism pathways. Among these operons, the pdhA, pdhC and pdhD encode pyruvate decarboxylase (E1 $\alpha$ ), dihydrolipoamide acetyltransferase (E2) and dihydrolipoamide dehydrogenase (E3) subunits of the pyruvate dehydrogenase complex

(Wang et al., 2013a). Compared with the control samples, the PdhC and PdhD subunits in the treatment samples were down-regulated by 0.79 fold and 0.52 fold, respectively, whereas, the PdhA subunit remained unchanged in 24 h. In addition, the PdhC subunit of *B. thuringiensis* with binding specifically to promoter regions can positively modify transcription of *cry1* class genes (Walter and Aronson, 1999). PdhC can also promote the formation of parasporal crystal by consuming a large amount of energy and material (Wang et al., 2013b). According to the specific function of these down-regulated proteins (Eno, TpiA, PdhC and PdhD), triclosan clearly inhibited the glycolytic metabolic pathway of *B. thuringiensis*, and which might even affect the synthesis of insecticidal crystal of *B. thuringiensis*. Perhaps this was also the self-regulation and repair of *B. thuringiensis* during the process of spore maturation. Although the presence of triclosan-induced linoleic acid damaged the membrane, the inhibition of the glycolytic metabolic process could promote the peptidoglycan synthesis, thereby preventing triclosan against *B. thuringiensis* membrane damage.

The proper protein folding in the protein synthesis process and quality controlling systems can ensure proteins display normal biological functions. Molecular chaperones and general proteolysis acts as two main strategic response to protein folding stress in bacteria (Molieri and Turgay, 2009). The molecular chaperon DnaK, owning the characteristics of refolding denatured protein and rescuing misfolded protein, is involved in the important chaperone protease systems of *B. thuringiensis* (Jiao et al., 2015). DnaK in *Bacillus pumilus* enhancing the output of recombinant protein, forming and disassembling protein complexes is an evidence to confirm the above mentioned function (Kumar et al., 2014). As a typical 70-kDa heat shock protein (Hsp70) in bacteria, DnaK induced the formation of a defense system in the presence of external stresses (Jiao et al., 2015) is another evidence for this inference.

The elongation factor G (FusA) can facilitate translational elongation by releasing the elongation-factor-G-guanosine diphosphate complex on the ribosome (Wang et al., 2013a). In this study, the synergetic down-regulated expression of FusA and ribosomal protein RplJ inhibited the protein synthesis in *B. thuringiensis*. The down-regulation

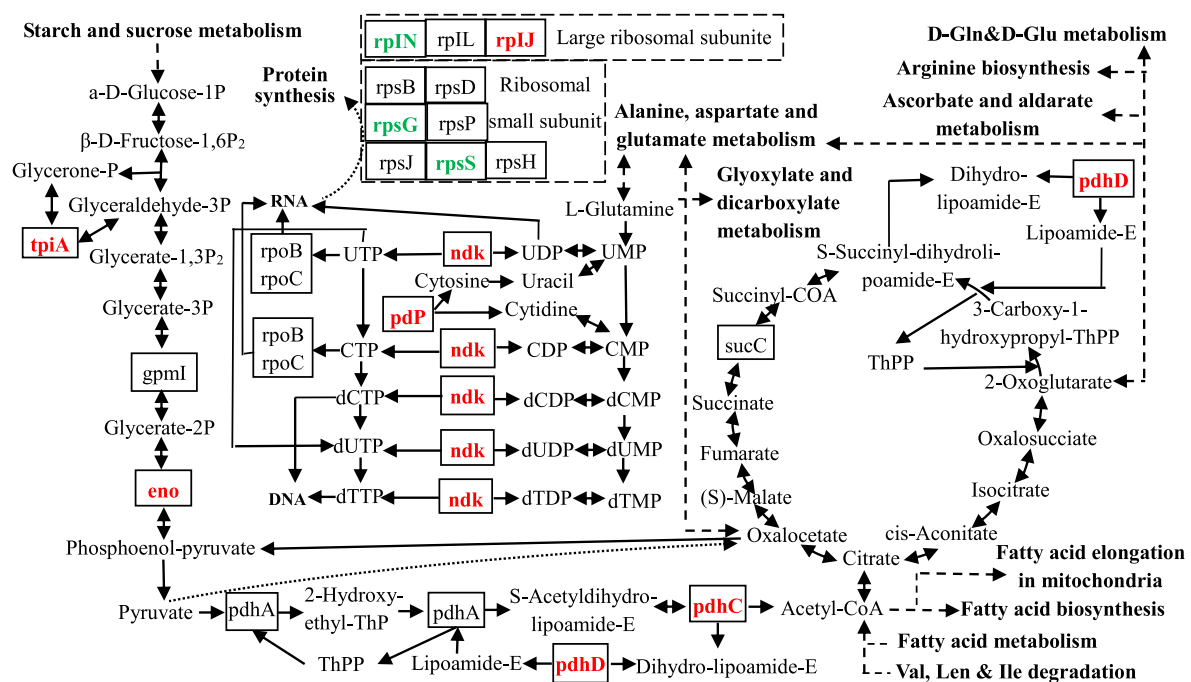


**Fig. 3.** Metabolic network catalyzed by differentially expressed proteins and other identified proteins. TpiA, GpmI, Eno, PdhA, PdhC and PdhD are involved in glycolysis; SucC and PdhD are involved in citrate cycle; Ndk, Pdp, RpoB and RpoC are involved in pyrimidine metabolism; RplN, RplL, RplJ, RpsB, RpsD, RpsG, RpsP, RpsJ, RpsS and RpsH are involved in ribosome metabolism. (Green indicates up-regulated protein, and Red stands for down-regulated protein.)

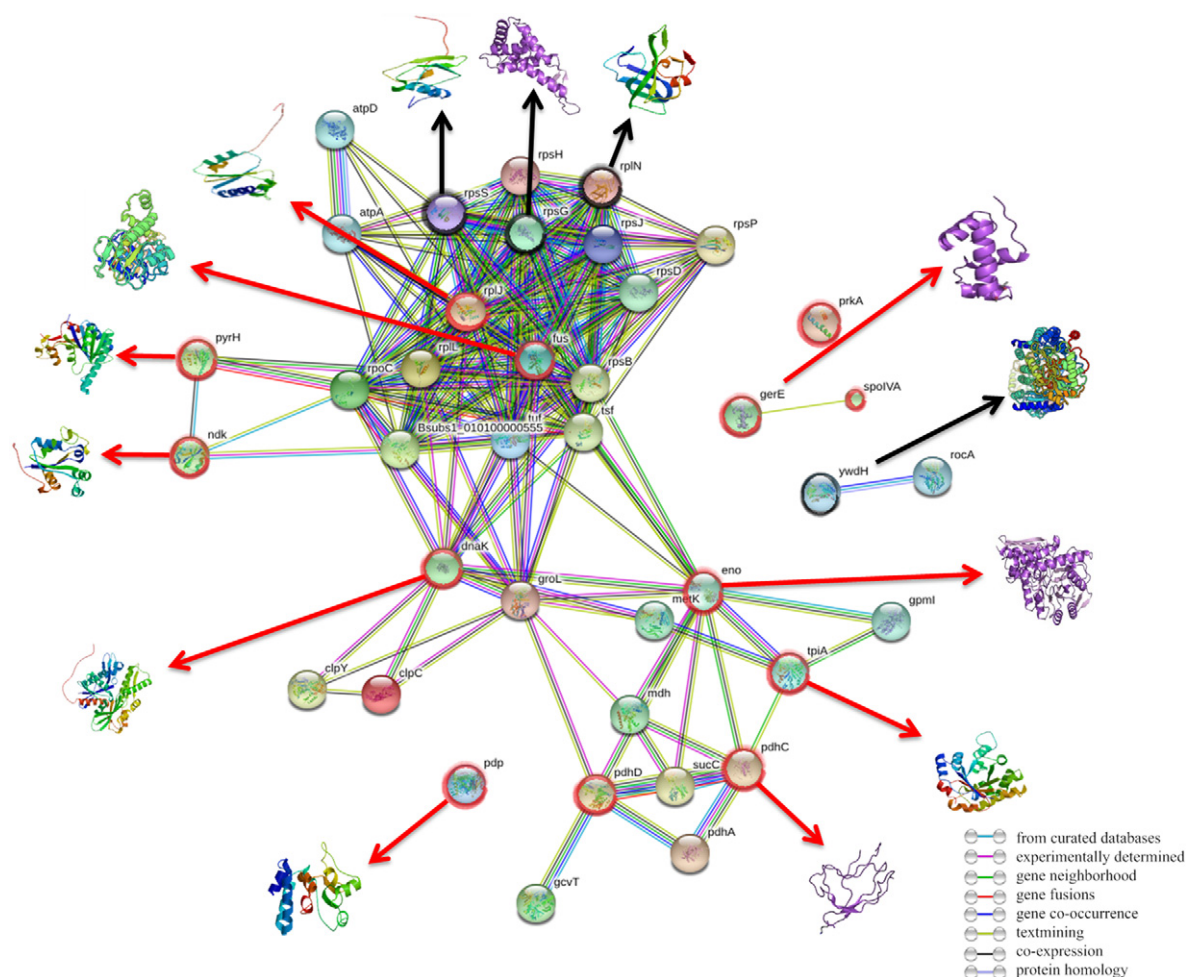


**Fig. 4.** Protein-protein interaction network between differentially expressed proteins and other identified proteins. The confidence score of protein-protein interaction network was set to high level  $> 0.7$ . The black circle represents the up-regulated proteins, while the red circle represents the down-regulated proteins. Arrows refer to the three-dimensional structures of protein.

of DnaK, FusA and RplJ involved in protein modification means that triclosan could hinder the repair and synthesis of the damaged proteins.

Nucleoside monophosphate kinases (PyrH) can catalyze the reversible transformation of nucleoside phosphate and nucleoside diphosphate for the synthesis of nucleic acids and nucleotidyl intermediates. As a member of this protein family only found in bacteria, PyrH with unique substrate characteristics becomes an ideal target of antimicrobial agents (Robertson et al., 2007). For example, PyrH has been reported to be a target for the inhibition of *Staphylococcus aureus* (Doig et al., 2013). That is why PyrH was used as an inhibited target biomolecule when new broad-spectrum antibiotics were developed (Ford et al., 2014). To further analyze the phylogenetic relationship of PyrH in different species, the amino acid sequences of PyrH from three species were obtained in the Uniprot database (Fig. 5). By sequence analysis of PyrH expressed in *B. thuringiensis* compared with *Staphylococcus aureus* and *Yersinia pestis*, the identification scores were 75.1% and 48.6%, respectively. This high similarity inferred that PyrH in *B. thuringiensis* could also be a target of triclosan stress based on its function and downward expression in the treatment sample.

The size and balance of the deoxynucleotide triphosphate (dNTP) pools determine the replication fidelity, while the imbalance of which will lead to an increase in mutagenesis. Nucleoside diphosphate kinase (Ndk), converting dNDP to dNTP, is involved in purine/pyrimidine metabolism and associated with the biosynthesis of DNA and RNA (Tabanelli et al., 2014). Based on the molecular function of Ndk in pyrimidine metabolism and protein synthesis, the expression of Ndk

under triclosan stress by qPCR was explored and validated in the present study (Table S4). The down-regulation of Ndk in qPCR validation was consistent with the proteomic results, which confirmed that the proteomic approach used in the current study is reliable. This finding provided a strong evidence that triclosan posed a threat to regulation of pyrimidine metabolism in *B. thuringiensis*. Besides, pyrimidine-nucleotides phosphorylase (Pdp) acts as an adjuvant enzyme involved in nucleotide salvage, catalyzing the reversible transfer of phosphate on the pyrimidine nucleotide glycoside (Szekei et al., 2012). The synergistic down-regulated expression of PyrH, Ndk and Pdp confirmed that triclosan inhibited the synthesis of DNA and RNA, whereas, this inhibitory effect was beneficial for providing carrier UDP to assist the transmembrane transport of peptidoglycan monomer.

Briefly, the effect of triclosan on the cellular metabolism of *B. thuringiensis* was mainly induced the down-regulation of proteins involved in the glycolytic and pyrimidine metabolic pathways, triggering the inhibitory effect on the synthesis of DNA/RNA and protein. The protein repair and energy metabolism were also suppressed. Whereas, the up-regulation of a small amount of ribosomal proteins, and the use of additional carbon nutrients and UDP were beneficial for the synthesis and transmembrane transport of peptidoglycan.

#### 3.4. Target biomolecule network related to triclosan stress

To reveal the biomarker network related to triclosan stress on human and other species, the target genes or proteins associated with

Bacillus_thuringiensis	. . . MSKPKYNRVVLKLSGEALAGEQGFGI NPTVI KSVAEQ	37
Staphylococcus_aureus	. . . NAQI SKYKRVVVLKLSGEALAGEKGFGI NPVI I KSVAEQ	38
Yersinia_pestis	MATNAKPVYQRI L LKLSGEALQGAEGFGI DASVLDRAQEQ	40
Bacillus_thuringiensis	VKEI AELDVEVA VVGGGNI WRGKI GSEMGMDRAGADYMG	77
Staphylococcus_aureus	VAEVAKMDCET AMI VGGGNI WRGKTGS DLGMDRGTADYMG	78
Yersinia_pestis	VKELVELGI QVGVVI GGGNLFRCAGLAQAGMNRVVGDFMG	80
Bacillus_thuringiensis	MLATVMNSLALQDSI ENI GI QTRVQTSI EMRQVAEPYI RR	117
Staphylococcus_aureus	MLATVMNALALQDSL EQLDCDTRVLTSL EMKQVAEPYI RR	118
Yersinia_pestis	MLATVMNGLANRDAL HRAYVNARLMSAI PLNGVCDNYSWA	120
Bacillus_thuringiensis	KAVRHLEKKRVVI FAAGTGNPYFSTDTTAAALRAAEI EADV	157
Staphylococcus_aureus	RAI RHLEKKRVVI FAAGI GNPYFSTDTTAAALRAAEVEADV	158
Yersinia_pestis	EAI SLLRHNRVVI FAAGTGNPFFTTDSAACLRGI EI EADV	160
Bacillus_thuringiensis	I LMAKNNVDGVYNADPSI DPTATKYETLTYLDVLKEGLCV	197
Staphylococcus_aureus	I LMGKNNVDGVYSADPKVNKDAVKYEH LTHI QMLQEGLCV	198
Yersinia_pestis	VLKAT. KVDGVYSADPVKNPDATLYEQLTYQDVLQEQLKV	199
Bacillus_thuringiensis	MDSTASSLCMDNDI PLI VFSVMEKGNI KRAVLGENI GTVV	237
Staphylococcus_aureus	MDSTASSFCMDNNI PLTVFSI MEEGNI KRAVMGEKI GTLI	238
Yersinia_pestis	MDLAAFTLARDHNLPI RVFNVNKPGALRRVVMGENE GTLI	239
Bacillus_thuringiensis	RG	239
Staphylococcus_aureus	TK	240
Yersinia_pestis	AK	241

**Fig. 5.** The amino acid sequences of PyrH from *B. thuringiensis*, *Staphylococcus aureus* and *Yersinia pestis*. Black indicates the consistency of the same sites between amino acid sequences. Cyan indicates that the similarity between the same sites in the amino acid sequence is high, and the yellow stands for that the similarity between the same sites of the amino acid sequence is low.

the response to triclosan stress were summarized in Table S5, and the metabolic network catalyzed by them was shown in Fig. 6. The main target metabolic pathways affected by triclosan were lipid metabolism, carbohydrate metabolism, nucleotide metabolism and amino acid metabolism, which was consistent with Fig. 3. To determine whether the same functional genes or proteins existed in human cells, the above target biomolecules found in previous papers and differential expressed proteins in the current study were analyzed in REACTOME database focusing on human biology. Fig. 7 clarified that these biomarkers were involved in fifteen pathways in human metabolic network, including immune system, signal transduction, development biology, metabolism of RNA, hemostasis, metabolism, transmembrane transport of small molecules, organelle biogenesis and maintenance, cellular responses to external stimuli, extracellular matrix organization, vesicle-mediated transport, protein metabolism, gene transcription, diseases and neuronal system, respectively. This finding illustrated the potential toxicity of triclosan to humans, especially RNA metabolism, organelle biogenesis and maintenance, cellular responses to external stimuli, gene expression and transcription. Thirty one branches in these pathways were screened out at  $P$ -values < 0.05 (Table S6) that could match the database statistically significantly. To further confirm whether the above results can correctly reflect the potential impacts of triclosan on human metabolism, the sequence homology of these proteins in non-human cells was compared with that of in human cells (Table S7).

Among these proteins, ACOX1, AHR, CAR, CYP1A, CYP1B1, DNMT1, ENO, HSP60, HSP70, SLC5A5, TPO and UGT found in human and other

species shared high percentage of homologous sequences confirmed that they did perform the same molecular function. This finding revealed that some target proteins found in other species could be biomarkers to reflect the metabolic impact on human cells, and the current proteomic study offered an insightful evidence of the potential impact of triclosan on human at molecule, pathway and network perspective.

### 3.5. Phylogenetic evolution of protein Eno

Eno in *B. thuringiensis* and *Homo sapiens* sharing high sequence homology illustrated that this protein could be a wide spectrum biomarker in different species to reflect the cellular response to stress. To confirm this inference, the phylogenetic relationship of Eno in prokaryotic and eukaryotic organisms was analyzed based on the amino acid sequences (Fig. 8). The result would reveal that the homologous correlation among various species, indicating the impact degree of triclosan on human and different target species.

These species, including *B. subtilis*, *Clonorchis sinensis* and *Haemonchus contortus* etc., were screened for homology analysis based on the similarity of amino acid sequences. The identification scores for all target species exceeded 40%, which validated the high homologous sequence of the protein Eno mentioned in the previous literature. This finding clarified that triclosan could be a disturbed compound to energy metabolism (Wang et al., 2014) and membrane recognition (Mundodi et al., 2008) of various species.



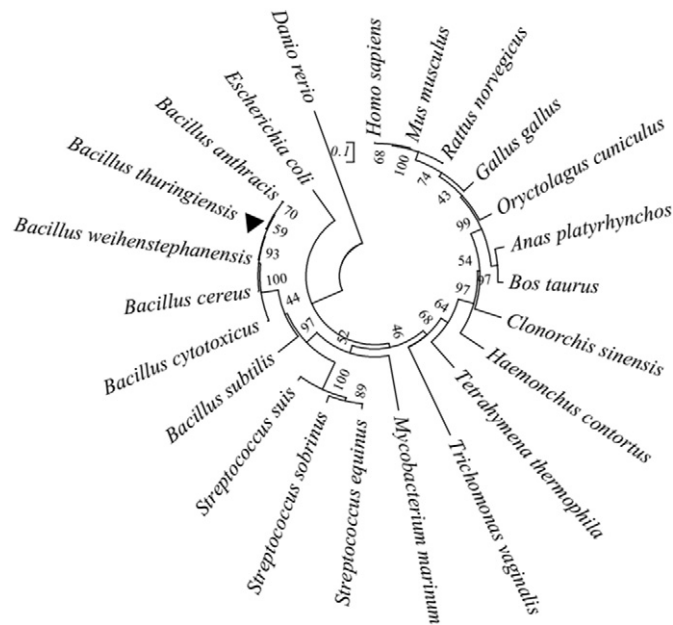


**Fig. 8.** Phylogenetic relationship of different species contained ENO. It was conducted by using the MEGA6.06 software according to the amino acid sequences of ENO. The numerical values represent the similarity of amino acid sequences among different species.

## Appendix A. Supplementary data

Supplementary data to this article can be found online at <https://doi.org/10.1016/j.scitotenv.2017.10.004>.

## References

- Amariei, G., Boltes, K., Rosal, R., Leton, P., 2017. Toxicological interactions of ibuprofen and triclosan on biological activity of activated sludge. *J. Hazard. Mater.* 334, 193–200.
- Axelstad, M., Boberg, J., Vinggaard, A.M., Christiansen, S., Hass, U., 2013. Triclosan exposure reduces thyroxine levels in pregnant and lactating rat dams and in directly exposed offspring. *Food Chem. Toxicol.* 59, 534–540.
- de Been, M., Francke, C., Moezelaar, R., Abeel, T., Siezen, R.J., 2006. Comparative analysis of two-component signal transduction systems of *Bacillus cereus*, *Bacillus thuringiensis* and *Bacillus anthracis*. *Microbiology* 152, 3035–3048.
- Bortner, C.D., Gomez-Angelats, M., Cidlowski, J.A., 2001. Plasma membrane depolarization without repolarization is an early molecular event in anti-Fas-induced apoptosis. *J. Biol. Chem.* 276, 4304–4314.
- Canesi, L., Ciacci, C., Lorusso, L.C., Betti, M., Gallo, G., Pojana, G., et al., 2007. Effects of triclosan on *Mytilus galloprovincialis* hemocyte function and digestive gland enzyme activities: possible modes of action on non target organisms. *Comp. Biochem. Physiol. Part C: Toxicol. Pharmacol.* 145, 464–472.
- Cornelius, F., 2001. Modulation of Na,K-ATPase and Na-ATPase activity by phospholipids and cholesterol. I. Steady-state kinetics. *Biochemistry* 40, 8842–8851.
- Dann, A.B., Hontela, A., 2011. Triclosan: environmental exposure, toxicity and mechanisms of action. *J. Appl. Toxicol.* 31, 285–311.
- Doig, P., Gorseth, E., Nash, T., Patten, A., Gao, N., Blackett, C., 2013. Screening-based discovery of the first novel ATP competitive inhibitors of the *Staphylococcus aureus* essential enzyme UMP kinase. *Biochem. Biophys. Res. Commun.* 437, 162–167.
- Feng, D.D., Luo, Z.Q., Roh, S.G., Hernandez, M., Tawadros, N., Keating, D.J., et al., 2006. Reduction in voltage-gated K<sup>+</sup> currents in primary cultured rat pancreatic beta-cells by linoleic acids. *Endocrinology* 147, 674–682.
- Ford, D.C., Ireland, P.M., Bullifant, H.L., Saint, R.J., McAlister, E.V., Sarkar-Tyson, M., et al., 2014. Construction of an inducible system for the analysis of essential genes in *Yersinia pestis*. *J. Microbiol. Methods* 100, 1–7.
- van Frankenhuyzen, K., 2009. Insecticidal activity of *Bacillus thuringiensis* crystal proteins. *J. Invertebr. Pathol.* 101, 1–16.
- Gaume, B., Bourgougnon, N., Auzoux-Bordenave, S., Roig, B., Le Bot, B., Bedoux, G., 2012. *In vitro* effects of triclosan and methyl-triclosan on the marine gastropod *Haliotis tuberculata*. *Comp. Biochem. Physiol. Part C: Toxicol. Pharmacol.* 156, 87–94.
- Jiao, L., Ran, J., Xu, X., Wang, J., 2015. Heat, acid and cold stresses enhance the expression of *DnaK* gene in *Alicyclobacillus acidoterrestris*. *Food Res. Int.* 67, 183–192.
- Kim, D., Pleumsamran, A., 2000. Cytoplasmic unsaturated free fatty acids inhibit ATP-dependent gating of the G protein-gated K<sup>+</sup> channel. *J. Gen. Physiol.* 115, 287–304.
- Kumar, M., Prasanna, R., Lone, S., Padaria, J.C., Saxena, A.K., 2014. Cloning and expression of *dnaK* gene from *Bacillus pumilus* of hot water spring origin. *Appl. Transl. Genomics* 3, 14–20.
- Levy, C.W., Roujeinikova, A., Sedelnikova, S., Baker, P.J., Stuitje, A.R., Slabas, A.R., et al., 1999. Molecular basis of triclosan activity. *Nature* 398, 383–384.
- Mayer, G., Heinze, G., Mischak, H., Hellemons, M.E., Heerspink, H.J.L., Bakker, S.J.L., et al., 2011. Omics-bioinformatics in the context of clinical data. In: Mayer, B. (Ed.), *Bioinformatics for Omics Data: Methods and Protocols*. 719, pp. 479–497.
- Meade, M.J., Waddell, R.L., Callahan, T.M., 2001. Soil bacteria *Pseudomonas putida* and *Alcaligenes xylosoxidans* subsp. denitrificans inactivate triclosan in liquid and solid substrates. *FEMS Microbiol. Lett.* 204, 45–48.
- Molieri, N., Turgay, K., 2009. Chaperone-protease systems in regulation and protein quality control in *Bacillus subtilis*. *Res. Microbiol.* 160, 637–644.
- Morohashi, M., Tsuchiya, K., Mita, T., Kawamura, M., 1991. Identification of (Na, K)ATPase inhibitor in brine shrimp, *Artemia salina*, as long-chain fatty acids. *J. Comp. Physiol. B.* 161, 69–72.
- Mundodi, V., Kucknoor, A.S., Alderete, J.F., 2008. Immunogenic and plasminogen-binding surface-associated alpha-enolase of *Trichomonas vaginalis*. *Infect. Immun.* 76, 523–531.
- Ordway, R.W., Singer, J.J., Walsh Jr., J.V., 1991. Direct regulation of ion channels by fatty acids. *Trends Neurosci.* 14, 96–100.
- Ortega-Anaya, J., Hernandez-Santoyo, A., 2016. Production of bioactive conjugated linoleic acid by the multifunctional enolase from *Lactobacillus plantarum*. *Int. J. Biol. Macromol.* 91, 524–535.
- Phan, T.-N., Marquis, R.E., 2006. Triclosan inhibition of membrane enzymes and glycolysis of *Streptococcus mutans* in suspensions and biofilms. *Can. J. Microbiol.* 52, 977–983.
- Robertson, D., Carroll, P., Parish, T., 2007. Rapid recombination screening to test gene essentiality demonstrates that *pyrH* is essential in *Mycobacterium tuberculosis*. *Tuberculosis* 87, 450–458.
- Silverio, S.C., Moreira, S., Milagres, A.M.F., Macedo, E.A., Teixeira, J.A., Mussatto, S.I., 2012. Interference of some aqueous two-phase system phase-forming components in protein determination by the Bradford method. *Anal. Biochem.* 421, 719–724.
- Szeker, K., Zhou, X., Schwab, T., Casanueva, A., Cowan, D., Mikhailopulo, I.A., et al., 2012. Comparative investigations on thermostable pyrimidine nucleoside phosphorylases from *Geobacillus thermoglucosidarius* and *Thermus thermophilus*. *J. Mol. Catal. B Enzym.* 84, 27–34.
- Tabanelli, G., Patrignani, F., Gardini, F., Vinderola, G., Reinheimer, J., Grazia, L., et al., 2014. Effect of a sublethal high-pressure homogenization treatment on the fatty acid membrane composition of probiotic lactobacilli. *Lett. Appl. Microbiol.* 58, 109–117.
- Tang, L., Wang, L., Ou, H., Li, Q., Ye, J., Yin, H., 2016. Correlation among phenyltins molecular properties, degradation and cellular influences on *Bacillus thuringiensis* in the presence of biosurfactant. *Biochem. Eng. J.* 105, 71–79.
- Treitz, C., Cassidy, L., Hoekendorf, A., Leippe, M., Tholey, A., 2015. Quantitative proteome analysis of *Caenorhabditis elegans* upon exposure to nematocidal *Bacillus thuringiensis*. *J. Proteome* 113, 337–350.
- Walter, T., Aronson, A., 1999. Specific binding of the E2 subunit of pyruvate dehydrogenase to the upstream region of *Bacillus thuringiensis* protoxin genes. *J. Biol. Chem.* 274, 7901–7906.
- Wang, J., Mei, H., Qian, H., Tang, Q., Liu, X., Yu, Z., et al., 2013a. Expression profile and regulation of spore and parasporal crystal formation-associated genes in *Bacillus thuringiensis*. *J. Proteome Res.* 12, 5487–5501.
- Wang, J., Mei, H., Zheng, C., Qian, H., Cui, C., Fu, Y., et al., 2013b. The metabolic regulation of sporulation and parasporal crystal formation in *Bacillus thuringiensis* revealed by transcriptomics and proteomics. *Mol. Cell. Proteomics* 12, 1363–1376.
- Wang, X., Chen, W., Tian, Y., Mao, Q., Lv, X., Shang, M., et al., 2014. Surface display of *Clonorchis sinensis* enolase on *Bacillus subtilis* spores potentializes an oral vaccine candidate. *Vaccine* 32, 1338–1345.
- Yang, M., Ye, J., Qin, H., Long, Y., Li, Y., 2017. Influence of perfluorooctanoic acid on proteomic expression and cell membrane fatty acid of *Escherichia coli*. *Environ. Pollut.* 220, 532–539.
- Ye, J., Liu, J., Li, C., Zhou, P., Wu, S., Ou, H., 2017. Heterogeneous photocatalysis of tris(2-chloroethyl) phosphate by UV/TiO<sub>2</sub>: degradation products and impacts on bacterial proteome. *Water Res.* 124, 29–38.
- Zhang, X., Candas, M., Griko, N.B., Rose-Young, L., Bulla, L.A., 2005. Cytotoxicity of *Bacillus thuringiensis* Cry1Ab toxin depends on specific binding of the toxin to the cadherin receptor BT-R-1 expressed in insect cells. *Cell Death Differ.* 12, 1407–1416.
- Zheng, C.J., Yoo, J.S., Lee, T.G., Cho, H.Y., Kim, Y.H., Kim, W.G., 2005. Fatty acid synthesis is a target for antibacterial activity of unsaturated fatty acids. *FEBS Lett.* 579, 5157–5162.